Morphology evolution and photoluminescence properties of ZnO films electrochemically deposited on conductive glass substrates

Bingqiang Cao, Weiping Cai,[a] Haibo Zeng, and Guotao Duan
Key Laboratory of Materials Physics and Anhui Key Laboratory of Nanomaterials and Nanostructures, Institute of Solid State Physics, Chinese Academy of Sciences, Anhui, Hefei 230031, People's Republic of China

(Received 13 September 2005; accepted 26 February 2006; published online 10 April 2006)

The current-dependent morphology evolution and photoluminescence properties of zinc oxide (ZnO) films prepared by electrochemical deposition (ECD) method were studied in this paper. It has been shown that the morphologies of ZnO films vary from porous to dense structure, from pillar crystal array to two-dimensional nanosheet covered film, with increase of deposition currents. Correspondingly, orientation of the film evolves from randomly to highly *c*-axis oriented structure. Current dependence of morphology is attributed to the ECD current-controlled preferential growth velocity along the *c* axis. All the ZnO films prepared over a wide current range show strong ultraviolet (UV) emission at room temperature, which also shows deposition current dependence in intensity, together with relatively weak defect-related green emission under UV excitations. Further experiments have revealed that a nonradiative relax process and a radiative electron-hole combination process are involved in this defect-related green emission and the excitonic origin of UV emission was also proved. © *2006 American Institute of Physics*. [DOI: 10.1063/1.2188132]

I. INTRODUCTION

Metal-oxide thin films (especially, wide and direct band gap semiconductors) are of great interest in optical and electronical industries, including blue and ultraviolet (UV) optical devices, such as light-emitting diodes and laser diodes.[1] ZnO, with a direct band gap of 3.37 eV and a high exciton binding energy of 60 meV at room temperature, is a kind of important technological semiconductor.[2] Since 1960s, preparations of ZnO film have been an active field because of their applications in sensors, actuators, resonators, and transparent electrodes for solar cells. Now most of the fabrication methods rely mainly on vacuum and physical/chemical vapor deposition technologies, such as metal-organic chemical vapor deposition (MOCVD),[3] molecular beam epitaxy (MBE),[4] magnetron sputtering (MR),[5] and pulsed laser deposition[6] (PLD) method. In these methods, special substrates with proper lattice parameters, such as gallium nitride,[3] *c*-plane sapphire,[4] or (001)-$LiNBO_3$ substrate,[6] are usually a prerequisite to reduce the strain at the interface. In view of the complex and energy-consuming experimental facilities mentioned above, increasing attentions have been paid on simple solution methods, including sol-gel method,[7] chemical bath deposition method,[8] spin coating method,[9] and electrochemical deposition (ECD) method[10] due to their benign environments and low cost in practical applications. ECD from dissolved aqueous solutions is an important low cost and scalable method that is well suited for the mass production of thin films on any conductive substrates. The film thickness, even morphologies and preferred orientations of many materials via ECD method, can be controlled by the deposition parameters. ECD of ZnO film was primarily demonstrated by Izaki and Omi[11] and Peulon and Lincot[12] ten years ago. However, crystal quality and physical properties of such film were not satisfactory. Then heteroepitaxial electrodeposition of ZnO films on some special substrates, such as single crystal gold,[13] GaN/sapphire,[14] and oriented-gold film coated silicon,[15] have been developed to improve the crystal quality and hence properties. For instance, room temperature UV photoluminescence (PL) has been observed recently in the oriented ZnO films electrodeposited on the oriented Au/Si substrate but the defect-related visible emission is still relatively strong.[15] As we know, ZnO films on transparent and conductive glass substrates are of wide applications in photovoltaic devices such as solar cells,[16] gas sensors,[17] and varistors.[18] However, there are only few reports on the ECD preparation method experimentally,[19–21] and their UV emission properties were rarely reported (only at low temperature).[22,23]

In this article, we study the morphological and structural evolutions of ZnO film, prepared by ECD method on conductive glass substrates, and their optical properties. It has been found that the film morphology and structure are strongly deposition current dependent, which varies from porous to dense structure, from pillar crystal array to two-dimensional (2D) nanosheet covered film with the increasing deposition currents. Correspondingly, orientation of the film evolves from nearly random to highly *c*-axis oriented structure. All the ZnO films prepared over a wide current range show strong UV emission at room temperature, which also shows deposition current dependent in intensity, together with relatively weak defect-related green emission. The simplicity and low-cost production of ZnO films with reproducible structural, morphological, and optical characteristics should be useful as a less expensive window material for practical industrial solar cell and display devices.

[a]Author to whom correspondence should be addressed; Fax: +86-551-5591434; electronic mail: wpcai@issp.ac.cn

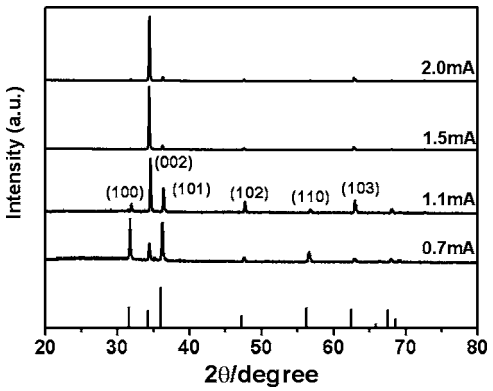

FIG. 1. XRD patterns of the ZnO film electrodeposited under different currents (vertical lines: JCPDS No. 36-1451).

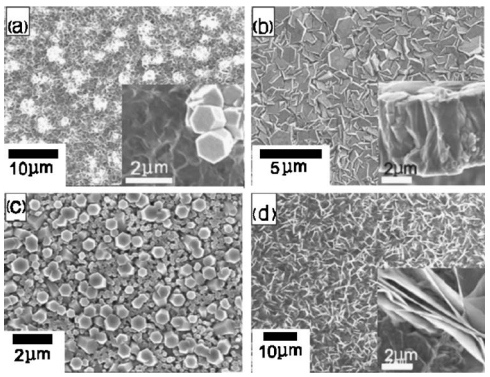

FIG. 2. SEM images show the surface microstructures of ZnO films electrodeposited under different ECD currents: (a) 0.7 mA; (b) 1.1 mA; (c) 1.5 mA; (d) 2.0 mA. Insets of (a) and (d): their corresponding enlarged SEM image. Inset of (b): its cross section SEM image.

II. EXPERIMENTAL DETAILS

Some commercial glass slides coated with a layer of 25 nm conductive indium-tin oxide (ITO) coated glass were used as the cathodes ($\sim 1\ cm^2$). The square resistance is about 150 $\Omega/\square$. Zinc sheets (99.99% purity) acted as the anode and the electrolyte was zinc nitrate aqueous solution ($0.05M$). Galvanostatic cathodic deposition was employed over a current range from 0.7 to 2.0 mA/cm^2. The deposition temperature was fixed at 70 °C by a water bath and the deposition time was 150 min for all samples. After the ECD experiments, the samples were washed and dried before further characterizations. The surface morphologies of the samples were observed by field emission scanning electron microscopy (FESEM, FEI Sirion 200). X-ray diffraction (XRD) was measured on Philips X'Pert diffractometer (40 KV, 40 mA)using Cu $K\alpha$ line (0.15419 nm). Raman scattering spectra were recorded on a LABRAM-HR Raman spectrometer excited with 514.5 nm Ar^+ laser and 325 nm He–Cd laser. PL properties were measured on a spectrometer (Jobin-Yvon) excited with 325 nm He–Cd laser, and on a FLS920 (EDINBURGH) fluorescence spectrophotometer excited with a Xe lamp or a nanosecond flash lamp, respectively.

III. RESULTS

A. Characterizations

Figure 1 shows the XRD spectra of the as-prepared films on ITO-glass substrates electrodeposited over a current range from 0.7 to 2.0 mA/cm^2. All the diffraction peaks of the films can be assigned to those of wurtzite ZnO phase (JCPDS: 36-1451). For the film deposited under a current of 0.7 mA/cm^2, the diffraction intensity ratio of the planes (100), (002), and (101) is similar to that of ZnO powders, indicating nearly randomly oriented grains in the film. For the films electrodeposited under a higher current, however, the significant {002} preferential orientation is exhibited, which is enhanced with increase of the deposition current.

Corresponding morphologies for the samples are illustrated in Fig. 2, showing significant dependence on the deposition current. When the deposition current is 0.7 mA/cm^2, the film shows a porous structured morphology [see Fig. 2(a)]. There are some hexagonal ZnO microcolumns, in accordance with the wurtzite crystal structure, embedded in the porous film [inset of Fig. 2(a)]. The film prepared under current of 1.1 mA/cm^2 [Fig. 2(b)] shows flat and compact surface morphology. It seems to be of many hexagonal nanosheets from the top view. However, cross-sectional observation [inset of Fig. 2(b)] indicates that such film is composed of densely aligned ZnO micropillars, which should have {002} preferential orientation combining the XRD results shown in Fig. 1. If the ECD current is 1.5 mA/cm^2, the film consists of highly aligned well-faceted hexagonal ZnO pillars [Fig. 2(c)], which has two size distributions (one is around 700 nm and the other is around 200 nm in size). They are not as compact as that shown in Fig. 2(b) but more strongly {002} preferential orientation. Further, when the cathodic current was increased to 2.0 mA/cm^2, the film surface was covered by 2D ZnO nanosheets with a thickness of tens of nanometers and a planar dimension of several micrometers, as shown in Fig. 2(d). From its enlarged SEM image [inset of Fig. 2(d)], we found that ZnO nanosheets are growing on the underneath ZnO microcolumns. This deposition current dependence of the film structure provides us a simple way to control the morphology and hence some related properties.

Further, Raman scattering spectra were measured due to its sensitivity to the crystallization, structural disorder, and defects in crystals. Figure 3 shows the result of the ZnO film

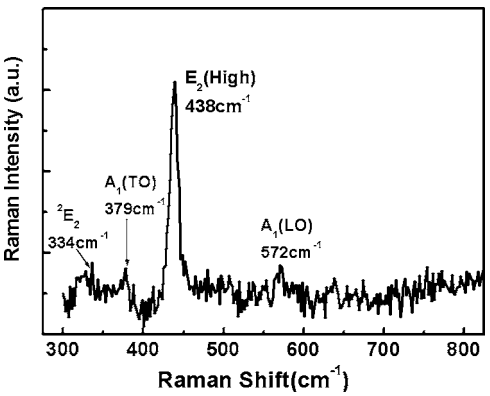

FIG. 3. Raman spectrum of the ZnO film electrodeposited under 1.5 mA excited by 514.5 nm Ar^+ laser.

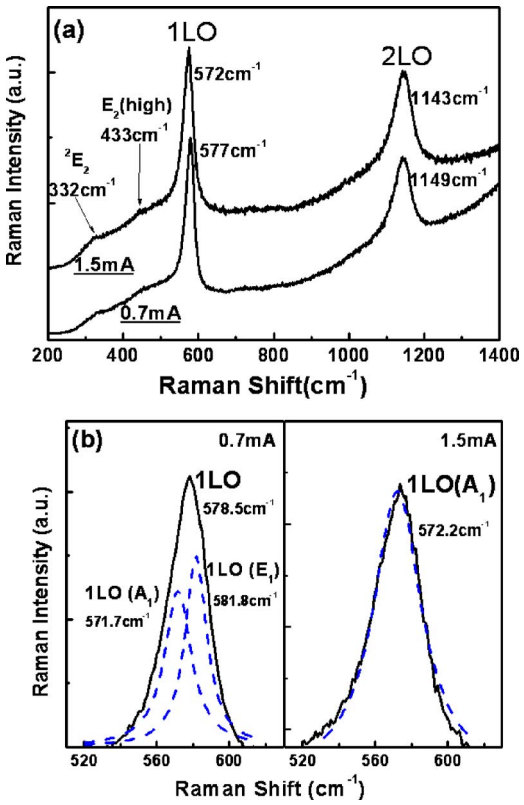

FIG. 4. (Color online) (a) Resonant Raman scattering spectra of the ZnO film under 0.7 and 1.5 mA excited by 325 nm He–Cd laser, respectively. [(b) and (c)]: Lorentzian curve fitting of the resonant 1LO Raman peaks of (a). (*n*LO refers to the *n*th longitudinal optical phonon mode.

deposited under 1.5 mA/cm^2 on the ITO-glass substrate excited with 514.5 nm Ar^+ laser. (The other samples show similar Raman spectra.) The characteristic wurtzite E_2 (high) mode at 438 cm^{-1}, and A_1 modes at 379 cm^{-1} (TO mode) and 572 cm^{-1} (LO mode) are observed, which is consistent with those observed in high quality ZnO film prepared by PLD method on sapphire substrate.[24] In addition, the Raman spectrum also shows a second-order Raman scattering $^2E_2$ mode at 334 cm^{-1}, which arises from zone-boundary phonon scattering.[25] The appearance of the characteristic Raman peaks confirms the wurtzite phase and good crystal quality for this ECD ZnO film.

Figure 4(a) shows the Raman spectra detected under the same backscattering geometric conditions as those in Fig. 3 but excited with 325 nm He–Cd laser for the 0.7 and 1.5 mA samples, respectively. We observed two strong peaks, respectively, centered at 572, 577 cm^{-1} and 1143, 1149 cm^{-1} for both samples, in addition to weak $^2E_2$ and E_2 (high) modes. The later peaks are at near twice frequency shifts of the formers. These two peaks can be attributed to the Raman 2LO and 1LO modes, respectively, due to the occurrence of resonant Raman scattering (RRS).[26] As we know, the LO mode is usually composed of A_{1LO} (574 cm^{-1}) mode and E_{1LO} (583 cm^{-1}) mode from polarization fields parallel and perpendicular to the *c* axis, respectively.[27] The Lorentzian curve fitting results [Fig. 4(b)] indicate that the 1LO mode of 0.7 mA film consists of both the A_{1LO} and E_{1LO} modes with comparable intensity, while that of 1.5 mA sample is only composed of the A_{1LO} mode together with undetectable E_{1LO}

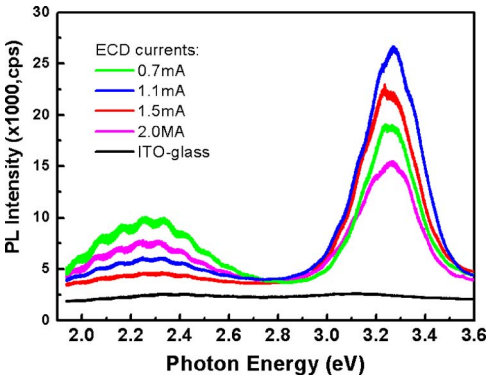

FIG. 5. (Color online) PL spectra of the as-synthesized ZnO films electrodeposited under different applied currents excited by He–Cd 325 nm lasers.

mode. According to the Raman selection rules,[28] if the wurtzite ZnO film is *c*-axis oriented, the E_1 (LO) mode is theoretically forbidden. So the absence of the E_{1LO} component in 1.5 mA film reveals its high {001} orientation, while the existence of both E_{1LO} and A_{1LO} components in 0.7 mA film indicates its randomly oriented structure, which is in accordance with the XRD results.

B. PL Measurements

The PL spectra excited by 325 nm He–Cd laser for all as-synthesized ZnO films are illustrated in Fig. 5, in which the result of the ITO-glass substrate is also presented for reference. All ZnO films show a typical UV emission peak centered at about 3.26 eV (380 nm), near the band edge of ZnO, in addition to a green emission centered around 2.3 eV (540 nm) in visible region. The intensity ratios of the UV to the green emission are about 2, 8, 15, and 3 for the samples deposited under currents of 0.7, 1.1, 1.5, and 2.0 mA/cm^2, respectively. These ratio values are comparable or close to those of the films prepared by plasma-assisted MBE method on sapphire substrate (about 10, under similar laser excitation conditions).[29] It indicates that such ECD ZnO films are of the similar crystal qualities to those prepared by vapor phase method. Obviously, deposition at 1.5 mA/cm^2 is the best in crystal qualities in this study.

For further study of the PL properties of such ZnO films, PL excitation (PLE) and time resolved PL spectra were also measured. Figure 6(a) shows the PL and PLE spectra of the 1.5 mA sample (as an example). At an excitation wavelength of 325 nm, we only detected a relatively weak and broad UV emission around 390 nm but no green emission, in contrast to the previous result for the ECD ZnO film on Au/Si substrate, which shows both UV (3.25 eV) and visible (2.80 eV) emissions with comparable intensities under similar xenon lamp excitation.[15] At an excitation of 350 nm, both the weak UV emission (around 390 nm) and the strong green emission (around 520 nm) were observed. If exciting at 375 nm, the green emission became much stronger. For the excitation spectrum corresponding to the 380 nm emission, there exist a peak around 325 nm. But for the excitation spectrum of the green emission centered at 525 nm, we can see a sharp excitonic absorption near the band gap edge (375 nm), indicat-

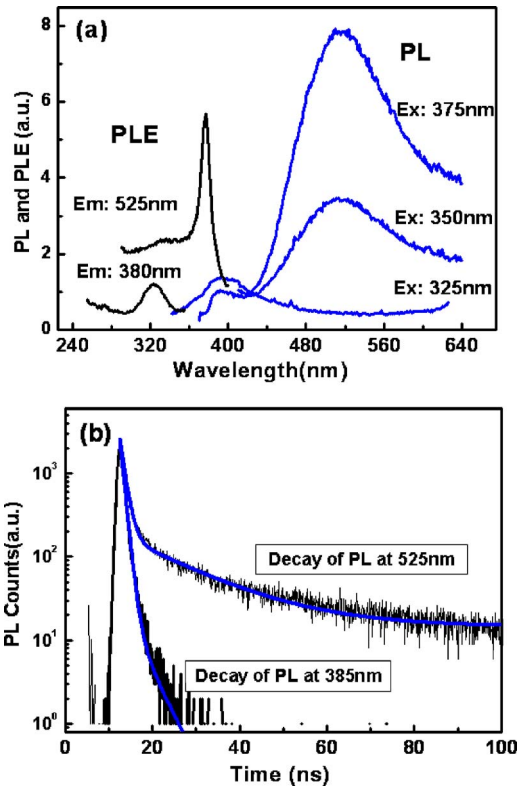

FIG. 6. (Color online) (a) PL and PLE spectra of ZnO film (1.5 mA) excited by different wavelength lights with a Xe lamp (b) TRPL spectra monitored at 380 and 525 nm of the ZnO film electrodeposited under a current of 1.5 mA.

ing that the main excitation mechanism for the green emission is electron-hole pair by interband absorption.

Figure 6(b) shows time resolved PL spectra of the 1.5 mA ZnO film monitored at wavelengths of 385 and 525 nm, respectively. The decaying parts of the both spectra can be well fitted by a biexponential decay function,

$$F = B_0 + B_1 \exp(-t/\tau_1) + B_2 \exp(-t/\tau_2), \quad (1)$$

where F is the intensity, and τ_1, τ_2 and B_1, B_2 are the decay time constants (lifetime) and their relative amplitudes, respectively. B_0 is the intensity fitting constant. These parameters and the relative fluorescence intensities (Φ) from the nonlinear least-square fitting are listed in Table I. The faster decaying ($\tau_1 = 0.83$ ns) component is dominant ($\Phi = 95\%$) for the UV emission. For the green emission, however, both the faster ($\tau_1 = 1.1$ ns) and slower ($\tau_2 = 15.6$ ns) decaying components are comparable in the relative fluorescence intensities.

TABLE I. Decaying parameters for the 1.5 mA ZnO film monitored at wavelengths of 385 and 525 nm, respectively. Note: Relative fluorescence intensity $\Phi_i = B_i\tau_i/(B_1\tau_1 + B_2\tau_2)$.

$F = B_0 + B_1 \exp(-t/\tau_1) + B_2 \exp(-t/\tau_2)$							
Ex (nm)	*Em* (nm)	τ_1 (ns)	Φ_1	τ_2 (ns)	Φ_2	B_2/B_1	χ^2
325	385	0.83	95%	3.78	5%	0.011	1.328
375	525	1.10	49%	15.6	51%	0.028	1.548

IV. DISCUSSIONS

A. Deposition current-dependent morphology

For the formation of ZnO, one-step cathodic electrochemical deposition reaction mechanism has been proposed.[30–32] From the chemical reaction point of view, with the reduction of nitrate ions and appearance of more hydroxyl ions in the electrolyte, the Zn^{2+} and OH^- ions will form $Zn(OH)_2$ on the cathode electrode. The deposited $Zn(OH)_2$ will subsequently be dehydrated and converted to ZnO at the temperature of the water bath (70 °C).

In fact, the nucleation and growth process of the ZnO are controlled by the ECD parameters, including cathodic potentials,[32] electrolyte,[11,12] and cathodic substrates,[13–15,33] In our cases, all ECD parameters are fixed except the deposition current. The ITO-glass substrate is amorphous in structure, which will not induce possible epitaxial relation with ZnO. It means that the randomly oriented nuclei will be formed on the substrate during the initial deposition. It is well known that ZnO is a polar crystal and produces positively Zn^{2+}-terminated (0001) and negatively O^{2-}-terminated $(000\bar{1})$ polar surfaces, which induce a net dipole moment along the c axis.[34] The surface energies of the polar {0001} planes are higher than those of nonpolar $\{01\bar{1}0\}$ and $\{2\bar{1}\bar{1}0\}$ planes.[35] So preferential growth along the c axis or [0001] direction is energetically favorable. In other words, {0001}-oriented ZnO nuclei will grow faster.

In the proper current range (say, from 1.1 to 1.5 mA), only {0001}-oriented ZnO nuclei grow preferentially along the c axis, leading to the films composed of {0001}-oriented hexagonal ZnO microrods [Figs. 2(b) and 2(c)]. Obviously, higher deposition current will correspond to the higher growth velocity ratio along the c axis to a axis. This is the reason that deposition at 1.5 mA/cm^2 results in noncompact film and nonflat film surface [see Fig. 2(c)], while the deposition at 1.1 mA/cm^2 forms compact and flat film [see Fig. 2(b)]. However, small deposition current (say, 0.7 mA) would induce more hydrogen liberation during ZnO formation,[36] which influences preferential growth and results in porous structure film in addition to few {0001}-oriented ZnO rods, as shown in Fig. 2(a). On the contrary, when the deposition current is very high (say, 2.0 mA), the corresponding film growth velocity is very high. Besides the oriented pillar crystal growth on the glass substrate, the newly formed ZnO would also nucleate on the preformed ZnO film, as shown in the inset of Fig. 2(d). But the newly formed ZnO then grew into 2D nanosheets. Obviously, such ZnO nanosheets are another form of anisotropy growth, which is different to that of the oriented film and energetically unfavorable in view of surface free energy. Illy *et al.*[37] have also observed ZnO nanosheets growing on polycrystalline zinc substrate and attributed this 2D growth to the close surface energy of one-dimensional (1D)/2D crystals under proper experimental conditions. But, in our ECD experiment, we think, this unique 2D anisotropy growth of the ZnO nanosheets is a fast nonequilibrium growth process caused by the high deposition currents.

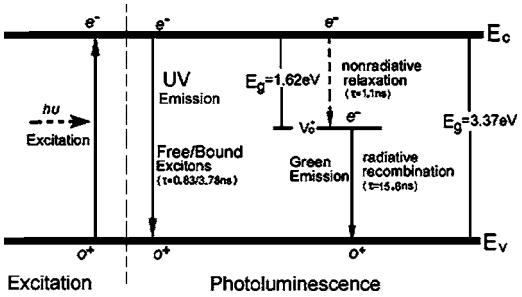

FIG. 7. Scheme of the UV/visible excitation and emission process.

B. Optical properties

It is commonly known that room temperature PL spectrum of ZnO usually shows three major peaks: one near band-edge UV emission peak centered at 380 nm and other two visible emissions localized in green or red region.[38] The UV peak is usually attributed to the excitonic emission, which is also confirmed in our experiment by the time resolved PL measurement that the dominant faster decay component ($\tau_1 = 0.83$ ns) can be ascribed to the radiative lifetime of excitons, similar to the values (0.86 and 0.97 ns) reported by Teke *et al.*[39] and Koida *et al.*[40] for single crystal ZnO at room temperature. Although the origin of the green emission is still controversial, it is generally accepted that it is related with the deep-level oxygen vacancy.[41,42] Furthermore, the fundamental carrier recombination dynamics of the green emission is not well understood. Based on our time resolved PL results, or the comparable biexponential behavior, we know that two different decays or capture processes should be involved in the visible emissions.[43] Considering that the visible emission is deep-level defect related, we suggest that the faster decaying constant (1.1 ns) represents the nonradiative transition process that the excited electrons at the bottom of the conduction band relax to deep-level defect states, such as oxygen vacancies, by a multiphonon process. An evidence for this conclusion is that this nonradiative relaxation process has the similar lifetime to that of the UV emission because the electrons in these two transition processes have the same initial states.[44] Then the slower decaying component (15.6 ns) must represent the radiative recombination of electrons and photoexcited holes in singly occupied oxygen vacancy states,[45] which is comparable to the radiative lifetime (14 ns) of trapped electrons and holes at surface states reported in CdSe nanoparticles.[46] Furthermore, the electrons relaxed to the deep defect levels cannot be reexcited to the conduction band by the thermal energy at room temperature, most of them will recombine with the holes in the valence band. So the nonradiative and radiative relative fluorescence intensities in the green emission are nearly equal. Figure 7 schematically illustrates the UV/green excitation and emission processes based on the above PL and time resolved PL spectra analysis.

V. CONCLUSIONS

In summary, we reported the ZnO film surface morphology evolution with deposition currents in the ECD on conductive glass substrates and studied their photoluminescence properties. Due to the high surface energies of the polar ZnO {0001} planes, there is a current window (from 1.1 to 1.5 mA/cm^2) that only {0001}-oriented ZnO nuclei grow preferentially along the *c* axis, leading to the films composed of {0001}-oriented hexagonal ZnO microrods. Higher deposition current will correspond to the higher ratio value of growth rate along the *c* axis to *a* axis, leading to a noncompact film with high crystal quality and hence strong UV emissions (high ratio of UV to visible emission). However, small deposition current results in porous structure film, due to significant hydrogen liberation during ZnO formation, which influences preferential growth. Too high deposition current leads to nanosheets grown on the film composed of micropillars due to the high deposition current-induced fast nonequilibrium growth. Such morphology-tuned ECD ZnO films show good UV emissions even at room temperature, especially for the noncompact and well-faceted ZnO nanorod array films prepared under current of 1.5 mA/cm^2. The fundamental carrier recombination dynamics of the UV and visible emissions are also discussed based on the PLE and time resolved PL spectra results. Our detailed studies could be helpful to understand the film ECD growth process and also afford an effective way to control the morphologies and even properties of the prepared films.

ACKNOWLEDGMENTS

We thank the National Natural Science Foundation of China (Grant No. 50271069) and National Project for Basic Research (Grant No. 2006CB300402) for their financial supports of this work. We also thank Dr. C. H. Ye (ISSP) for his fruitful discussions with us.

[1] R. F. Service, Science **276**, 895 (1997).
[2] D. C. Look, Mater. Sci. Eng., B **80**, 383 (2001).
[3] Th. Gruber, C. Kirchner, and A. Waag, Phys. Status Solidi B **229**, 841 (2002).
[4] Z. K. Tang, G. K. L. Wong, P. Yu, M. Kawasaki, A. Ohtomo, H. Koinuma, and Y. Segawa, Appl. Phys. Lett. **72**, 3270 (1998).
[5] T. Yamamoto, T. Shiosaki, and A. Kawabata, J. Appl. Phys. **51**, 3113 (1980).
[6] G. H. Lee, Solid State Commun. **128**, 351 (2003).
[7] Y. Zhang, B. X. Lin, X. K. Sun, and Zh. X. Fu, Appl. Phys. Lett. **86**, 131910 (2005).
[8] M. Izaki, Chem. Commun. (Cambridge) **5**, 476 (2002).
[9] M. Berber, V. Bulto, R. Kliß, and H. Hahn, Scr. Mater. **53**, 547 (2005).
[10] A. G. H. Therese and P. V. Kamath, Chem. Mater. **12**, 1195 (2000).
[11] M. Izaki and T. Omi, Appl. Phys. Lett. **68**, 2439 (1996).
[12] S. Peulon and D. Lincot, Adv. Mater. (Weinheim, Ger.) **8**, 166 (1996).
[13] R. Liu, A. A. Vertegel, E. W. Bohannan, Th. A. Sorenson, and J. A. Switzer, Chem. Mater. **13**, 508 (2001).
[14] Th. Pauporté and D. Lincot, Appl. Phys. Lett. **75**, 3817 (1999).
[15] M. Izaki, S. Watase, and H. Takahashi, Adv. Mater. (Weinheim, Ger.) **15**, 2000 (2003).
[16] T. Yoshida, M. Tochimoto, D. Schlettwein, D. Wöhrle, T. Sugiura, and H. Minoura, Chem. Mater. **11**, 2657 (1999).
[17] M. L. de la Olvera and R. Asomoza, Sens. Actuators B **45**, 49 (1997).
[18] S. Ezhilvalavan and T. R. N. Kutty, Mater. Chem. Phys. **49**, 258 (1997).
[19] Z. H. Gu and T. Z. Fahidy, J. Electrochem. Soc. **146**, 156 (1998).
[20] M. Izaki, J. Electrochem. Soc. **146**, 4517 (1999).
[21] J. Weng, Y. J. Zhang, G. Q. Han, Y. Zhang, L. Xu, J. Xu, X. F. Huang, and K. J. Chen, Thin Solid Films **478**, 25 (2005).
[22] Th. Pauporté and D. Lincot, Electrochim. Acta **45**, 3345 (2000).
[23] D. G. Kim, T. Terashita, I. Tanaka, and M. Nakayama, Jpn. J. Appl. Phys., Part 2 **42**, L935 (2003).
[24] C. Roy *et al.*, Thin Solid Films **436**, 436 (2003).

[25]M. Rajalakshmi, A. K. Arora, B. S. Bendre, and S. Mahamuni, J. Appl. Phys. **87**, 2445 (2000).
[26]J. M. Calleja and M. Cardona, Phys. Rev. B **16**, 3753 (1977).
[27]J. F. Scoot, Phys. Rev. B **2**, 1209 (1970).
[28]Y. Zhang, H. B. Jia, R. M. Wang, C. P. Chen, X. H. Luo, D. P. Yu, and C. I. Lee, Appl. Phys. Lett. **83**, 4631 (2003).
[29]Y. F. Chen, D. M. Bagnall, H. J. Koh, K. T. Park, K. Hiraga, Z. Q. Zhu, and T. Yao, J. Appl. Phys. **84**, 3912 (1998).
[30]S. Peulon and D. Lincot, J. Electrochem. Soc. **145**, 864 (1999).
[31]Y. J. Lee and Y. S. Tak, Electrochem. Solid-State Lett. **4**, C63 (2001).
[32]B. Q. Cao, W. P. Cai, F. Q. Sun, Y. Li, Y. Lei, and L. D. Zhang, Chem. Commun. (Cambridge) **14**, 1604 (2004).
[33]B. Q. Cao, F. Q. Sun, and W. P. Cai, Electrochem. Solid-State Lett. **8**, G237 (2005).
[34]Z. L. Wang, X. Y. Kong, and J. M. Zou, Phys. Rev. Lett. **91**, 185502 (2003).
[35]Z. L. Wang, J. Phys.: Condens. Matter **16**, R829 (2004).
[36]P. K. Shen, N. Chi, and K. Y. Chan, J. Mater. Chem. **10**, 697 (2000).
[37]B. Illy, B. A. Shollock, J. L. M-Driscoll, and M. P. Ryan, Nanotechnology **16**, 320 (2005).
[38]X. Liu, X. H. Wu, H. Cao, and R. P. H. Chang, J. Appl. Phys. **95**, 3141 (2004).
[39]A. Teke, Ű. Özgűr, S. Doğan, X. Gu, H. Morkoç, B. Nemeth, J. Nause, and H. O. Everitt, Phys. Rev. B **35**, 8281 (1987).
[40]T. Koida, S. F. Chichibu, A. Uedono, A. Tsukazaki, M. Kawasaki, T. Sota, Y. Segawa, and H. Koinuma, Appl. Phys. Lett. **82**, 532 (2003).
[41]K. Vanheusden, C. H. Seager, W. L. Warren, D. R. Tallant, and J. A. Voigt, Appl. Phys. Lett. **68**, 403 (1996).
[42]S. B. Zhang, S.-H. Wei, and A. Zunger, Phys. Rev. B **63**, 075205 (2001).
[43]C. H. Ye, X. S. Fang, G. H. Li, and L. D. Zhang, Appl. Phys. Lett. **85**, 3035 (2004).
[44]*Photoluminescence of Solids* (University of Science and Technology of China Press, Hefei, 1980), p. 449.
[45]K. Vanheusden, W. L. Warren, C. H. Seager, D. R. Tallant, J. A. Voigt, and B. E. Gnade, J. Appl. Phys. **79**, 7983 (1996).
[46]P. Levebvre, H. Mathieu, J. Allègre, T. Richard, A. Combettes-Roos, M. Pauthe, and W. Granier, Semicond. Sci. Technol. **12**, 958 (1997).